PASSIVE MICROWAVE STUDIES

by

James P. Hollinger
E. O. Hulburt Center for Space Research
Naval Research Laboratory
Washington, D. C. 20390

INTRODUCTION

The microwave oceanography project is supported by the Spacecraft Oceanography Project Office (SPOC) of the U. S. Naval Oceanographic Office. The objective is to determine, through a measurement program, the optimum system parameters, measurement techniques and understanding of physical phenomena to enable unambiguous all-weather determination of the sea surface properties of sea roughness, surface wind fields, temperature, salinity, sea ice, and pollution by means of remote passive microwave sensing from a satellite. The program is primarily concerned with aircraft-borne observations; however, extensive measurements have also been made from a fixed ocean platform. Both platforms have their own distinct advantages and complimentary information may be obtained by utilizing the special characteristics of each. The aircraft program will be discussed first, and then the results of observations from Argus Island tower will be described.

AIRCRAFT MEASUREMENT PROGRAM

All of our aircraft measurements have been made with the multifrequency microwave radiometer (MFMR) system aboard the NASA MSC P-3 aircraft. The aircraft platform has the advantages, compared to near surface measurements, of spatial resolutions, data acquisition rates, and atmospheric conditions more nearly comparable to those encountered from a satellite. In addition, these properties may be varied to some extent by adjusting the aircraft altitude and the aircraft allows a wide range of sea conditions to be pursued. Since the Earth Resources Review last year, we have participated in four missions. Mission 113 over the Gulf of Mexico in November 1969 was flown primarily to evaluate the MFMR, which had just

been installed in the P-3, and to set up procedures and techniques for the first Joint Ocean Surface Study (JOSS I) as well as to obtain some preliminary sea state data. Extensive sea state measurements were made during Mission 119 off Bermuda in January 1970 as part of JOSS I. Sea ice observations were made as part of Mission 126 off Alaska in April 1970 and salinity effects were studied in the Columbia River plume in August 1970 in connection with Mission 140. Good data were obtained from all of these missions except Mission 126 when poor weather prevented flights over the desired ice conditions. The data from these missions are very nearly reduced but are not yet in final form for analysis and it is not possible to report the results at this meeting. We have worked closely with and had excellent cooperation from the Earth Resources Division in the testing and calibration of the MFMR and in preparing the computer reduction programs. We hope to have the final results in the very near future. In fact a large measure of our program next year will be the analysis and interpretation of the MFMR data taken to date.

TOWER MEASUREMENT PROGRAM

OBJECTIVE

The tower measurements were undertaken to investigate the effects of sea state on the microwave brightness temperature of the sea surface. The fixed ocean platform provides the advantages of high spatial resolution on the sea surface, excellent ground truth, and a relative ease of radiometer calibration and determination of antenna characteristics as compared to an aircraft platform. In addition, there is no correction necessary for radome or atmospheric loss between the antenna and the sea. The microwave brightness temperature dependence on sea state (wind speed) arises from two effects. The first effect results from the increasing roughness of the compact water surface and the second effect from the increasing coverage of white caps and sea foam with increasing wind speed. Although both are properly termed roughness effects, the first will be referred to as the surface roughness effect, and the second as the sea foam effect. The high spatial resolution of the sea surface available from the ocean tower allows these two effects to be studied separately.

Surface roughness has been investigated theoretically using a geometric optics model (1) based on the sea surface slope distribution of Cox and Munk (2) and using a physical optics model (3) which depends upon the correlation function of the surface heights. Multiple-scatter and shadowing effects which become important at large angles of incidence have been investigated using a one dimensional geometric optics model (4). The very high microwave brightness temperature of sea foam compared to the average sea surface, which results in the sea foam effect, was first suggested by Williams (5) and has been supported theoretically on the basis of a physical model for foam (6). Measurements of the microwave brightness temperature of the sea surface (7), (8), (9), (10) indicate a dependence on surface roughness and sea foam which is correlated with wind speed. However more measurements are needed over a wide range of sea conditions with accompanying ground truth and as a function of the observational parameters of frequency, polarization, and incidence angle to understand and interpret the microwave emission of the sea in terms of the properties of the sea surface.

OBSERVATIONS

The measurements to be described were made from Argus Island tower at 1.41, 8.36, and 19.34 GHz in March 1970. Also included are the results of observations at 8.36 and 19.34 GHz made in March-April 1969 (8). Argus Island is located approximately 45 km southwest of Bermuda in 60 meters of water. Each microwave radiometer consists of a parabolic antenna and linearly-polarized feed system followed by a conventional Dicke-type crystal-mixer superheterodyne receiver. The Dicke-switch alternately connects the receiver input to the antenna and to an ambient matched waveguide termination whose temperature is accurately known to allow the absolute antenna temperature of the incident linearly-polarized radiation to be measured. Since the antennas can be rotated about their electrical axes, any plane of linearly polarization may be measured. In practice, the vertical and horizontal components were measured. The rms noise output fluctuations with the 1-sec integration time constant used at 1.41, 8.36, and 19.34 GHz are respectively 1/2, 1/4, and 1/2°K and half-power beamwidths are 4.7, 3.4, and 2.7 degrees; this provides a resolution on the sea surface at nadir of about 2.2, 1.2, and 0.9 meters.

Average antenna temperatures were measured by integrating the radiometer output, as successive waves passed through the beam, until a stable value was obtained, usually one to two minutes. Measurements were made at a series of incremented incidence angles. Increments of 5 or 10 degrees were chosen depending on the rate of change of antenna temperature with incidence angle. The relatively high microwave brightness temperature of sea foam compared to the general surface made it easy to recognize the signal produced by a white cap or foam patch of size comparable to or larger than the spatial resolution on the sea surface. These white caps were excluded from the antenna temperature average. Although very thin or small patches could not be individually recognized and removed, it is believed that the majority of white caps were eliminated and that the measured antenna temperature is primarily due to surface roughness effects.

The atmospheric opacity at the time of each sea measurement was determined by atmospheric emission measurements between the zenith and the horizon (11). The measured antenna temperatures were corrected for spurious radiation entering the side and back lobes of the antenna and a partial correction for sky radiation reflected from the sea was made to obtain the brightness temperature of the sea averaged over the main beam of the antenna. In order to correct completely for reflected sky radiation, the differential scattering coefficients of the sea surface must be known (12). Since they are not known, a "first order" correction was made using the average measured emissivity of the sea to obtain the sea reflectivity and assuming specular reflection of the sky radiation. This correction removes the bulk of the reflected sky radiation. However, it is only accurate for smooth seas and becomes poorer as the sea roughens and large angle scattering increases. It also becomes progressively worse at larger incidence angles where the reflected sky radiation is largest and multiple-reflection and shadowing are most severe. Therefore the measured brightness temperature contains a small residual reflected sky component which is dependent upon the atmospheric opacity and sea surface roughness. The absolute errors in antenna temperature and the relative errors in brightness temperature are about $\pm 2\,^{\circ}K$. The absolute errors in brightness temperature are about 5 to 10 percent.

The sea states encountered during the measurements ranged from calm to wind speeds of nearly 15 m/sec and

significant wave heights of from 1.2 to 2.3 meters. The sea was never specular nor fully developed. Swell was present even for no wind. In one 24-hour period, the wind direction moved around the compass as the wind speed changed from calm to 14 m/sec. The wind speeds were recorded at a height of 43.3 meters above the sea surface. The sea temperature was 291° ± 1°K and the salinity 35 °/₀₀ ± 1 °/₀₀ for all the observations.

RESULTS AND DISCUSSION

To define the change of brightness temperature with incidence angle and with sea conditions, two groups of data at the upper and lower ends of the wind speeds encountered were selected and averaged together. The two groups represent average wind speeds of 0.5 and 13.5 m/sec. No wind speed for data runs used in either group differs from the average for the group by more than 1 m/sec. Figure 1 shows the brightness temperature of the vertical and horizontal components for these two groups at 1.41, 8.36, and 19.34 GHz as a function of incidence angle. Also shown for comparison purposes are the brightness temperatures calculated for wind speeds of 0 and 15 m/sec using the theoretical geometric optics model developed by Stogryn (1). The dielectric constant of sea water used in the calculations is based on the data of Saxton and Lane (13) and the sky opacity used is the average of the values determined at the time of the observations. The calm sea contribution to the reflected sky radiation has been removed in order that the calculations most nearly correspond to the measured brightness temperatures. The data show that the vertical component is independent of wind speed in the region of 55 degrees incidence angle and increases below and decreases above this angle with increasing wind speed. The horizontal component increases with wind speed over the range of incidence angle from 20 to 70 degrees with a slightly greater increase at the larger incidence angles. The wind speed dependence of the horizontal component generally is greater than that of the vertical component. There is a marked decrease in wind speed dependence with decreasing observational frequency. Except for slight shifts in absolute level which are probably due to errors in absolute calibration, the data is in qualitative agreement with the theoretical calculations. The two biggest differences between the calculations and the measurements are that the theory predicts very little dependence on

observational frequency and a much smaller wind speed dependence of the horizontal component at small incidence angles. This later discrepancy was first pointed out by Nordberg et al. (7) and indicated by previous measurements (8). The failure of the geometric optics model to account for the observational frequency dependence results from the fact that only the dielectric constant of the sea water and the atmospheric opacity are frequency dependent in the model and they primarily affect only the absolute level.

Figure 2 shows the individual measurements of the vertical and horizontal components and the percentage polarization, defined as the ratio of the difference of these two components to their sum, at 55 degrees incidence angle as a function of wind speed. The solid lines are linear least-square solutions fitted to the data. As before, the vertical component is seen to be independent of wind speed and the horizontal component shows a marked decrease in wind speed dependence with decreasing observational frequency. The dependence at 1.41 GHz is only about 1/3 of its value at 19.34 GHz.

To summarize the measurements for all incidence angles most concisely least-square straight lines have been fitted to the data at each incidence angle and the slopes of the lines plotted versus incidence angle in Figure 3. The dotted lines indicate the error in the slope determination. The wind speed independence of the vertical component in the region of 55 degrees incidence angle at all frequencies and the decrease in wind speed dependence of the horizontal component with decreasing incidence angle are apparent. The percentage polarization is dependent on sea surface roughness; decreasing with increasing wind speed. It has the desirable advantage for a spacecraft-borne sensor that it is practically independent of errors in absolute calibration.

Because the atmospheric opacity decreases with decreasing frequency and the measured brightness temperature contains an atmospheric opacity dependent sky reflection component, some decrease in the wind speed dependence of the brightness temperature with frequency is to be expected. In order to estimate what fraction is due to changes in the effective emissivity of the sea and what is due to variations in the reflected sky radiation, the differential scattering coefficients of the sea surface were calculated using the geometric optics model developed by Stogryn (1). This model was chosen because it explicitly contains the wind speed

dependence through the Cox and Munk (2) sea surface slope distribution and is in rough agreement with the data at larger incidence angles. In the calculations the average of the opacities determined during the observations of 0.009, 0.017, and 0.069 nepers at 1.41, 8.36, and 19.34 GHz respectively were used. The range in opacities during the observations was negligible at 1.41 GHz and ± 17% and ±33% at 8.36 and 19.34 GHz respectively. These calculations of the differential change in horizontal brightness temperature at 55 degrees incidence angle as a function of wind speed are given in Figure 4. The upper curve is the sum of the calculated wind speed dependence of the radiation emitted by the sea and the wind speed dependent part of the reflected sky radiation. The crosshatched area represents the wind speed dependent reflected sky component. The measured values of the horizontal brightness temperature at 55 degrees incidence angle expressed as differentials above the zero wind speed intercept of the least square line given in Figure 2 are also shown. The calculated sky component is, as expected, greater at higher frequencies. But even at 19.34 GHz, except at low wind speeds, the emitted component is dominant. Thus the geometric optics model indicates that the observed dependence of microwave brightness temperature on wind speed is primarily due to changes in the effective emissivity of the sea surface. The exact separation of the emitted and reflected components is model dependent and a definitive conclusion is not possible until a fully acceptable theory is developed. Depending upon which component is dominant, an observational frequency could be chosen to maximize the wind speed dependent signal. In either case, for remote sensing of sea state, the atmospheric opacity would have to be determined to some degree to allow the received signal to be corrected for the wind speed independent part of reflected sky radiation and the effects of the atmosphere between the sensor and the sea.

The measurements shown in Figure 4 are in fair agreement with the model at 19.34 GHz but the agreement is progressively worse at the two lower frequencies. Since the model calculations depend on the mean square slope of the sea surface, the slope of the calculated curves would be reduced by chosing a smaller value than that given by Cox and Munk. A reasonable fit to the measurements is obtained if mean square slopes of about 1/3, 1/2, and 2/3 of the mean square slope given by Cox and Munk are used at 1.41, 8.36, and 19.34 GHz respectively. Cox and Munk found that the presence of an oil slick reduced the mean

square slope with respect to a clean surface by a factor of two or three which is comparable to the reduction from 19.34 GHz to 1.41 GHz. In addition they calculated (14) that an oil slick damped waves of 0.3 m wavelength by a factor of 10 and that waves shorter than this were essentially eliminated. Thus a possible interpretation of the reduction of mean square slope with decreasing frequency required to fit the observations is that waves shorter than the observational wavelength are unimportant in determining the microwave properties of the sea surface. The adjustment of mean square slope in Stogryn's geometric optics model to fit the observations is analogous to Wright's (15) use of steeper surface tilts with increasing frequency to interpret radar backscatter observations in terms of Bragg scattering. In addition the persistence of the wind speed dependence of the brightness temperature over arbitrary wind and sea directions and wind duration and fetch, as well as the relatively small variation in significant wave height during the observations, implies a close coupling between wind speed and the sea roughness features controlling the microwave properties. This indicates that the very long waves are not of primary importance in determining the microwave properties of the sea. Certainly a frequency dependent model is required to explain the microwave brightness temperature of the rough sea surface.

CONCLUSIONS

Observations of the microwave brightness temperature of the sea show a definite dependence on wind speed. This dependence is due to roughness effects of the compact surface associated with wind-driven waves. The wind speed dependence decreases with observational frequency and any theoretical model used to interpret the microwave characteristics of the sea must be frequency dependent. The frequency dependence may be interpreted on the basis of a geometric optics model (1) as a relative unimportance of surface waves shorter than the observational wavelength in determining the microwave properties of the sea surface.

Surface roughness effects will dominate at the lower wind speeds. But due to the increasing prevalence of sea foam with increasing sea state (16) and the high microwave brightness temperature of foam, the microwave characteristics of the sea will be determined by sea foam at very

high wind speeds (9), (10). The transition wind speed between the two effects is not known but will probably lie in the region between 10 and 15 m/sec.

REFERENCES

(1) Stogryn, A. IEEE Trans. Antennas and Propagation, vol. AP-15, pp. 278-286, March 1967.

(2) Cox, C. and Munk, W. J. Opt. Soc. Am., vol. 44, pp. 838-850, November 1954.

(3) Ulaby, F. T. and Fung, A. K. Southwest IEEE Conf. Proc., pp. 436-440, April 1970.

(4) Lynch, P. J. and Wagner, R. J. J. Math. Phys., vol. 11, pp. 3032-3042, October 1970.

(5) Williams, G. F., Jr. J. Geophys. Res., vol. 74, pp. 4591-4594, August 20, 1969.

(6) Droppleman, J. D. J. Geophys. Res., vol. 75, pp. 696-698, January 20, 1970.

(7) Nordberg, W., Conaway, J., and Thaddeus, P. Q. J. Royal Met. Soc., vol. 95, pp. 408-413, April 1969.

(8) Hollinger, J. P. J. Geophys. Res., vol. 75, pp. 5209-5213, September 20, 1970.

(9) Ross, D. B., Cardone, V., and Conaway, J. IEEE Trans. Geoscience and Electronics, vol. GE-8, (in press) October 1970.

(10) Nordberg, W., Conaway, J., Ross, D. B, and Wilheit, T. J. Atmos. Sci. (in press).

(11) Dicke, R. H., Beringer, R., Kyhl, R. L., and Vane, A. B. Phys. Rev., vol. 70, pp. 340-348, September 1 and 15, 1946.

(12) Peake, W. H. IRE Trans. Antennas and Propagation (Special Suppl.), vol. AP-7, pp. S324-S329, December 1959.

(13) Saxton, J. A. and Lane, J. A. Wireless Engineer, vol. 29, London: Dorset House, pp. 269-275, October 1952.

(14) Cox, C. and Munk, W. J. Marine Res., vol. 13, pp. 198-227, 1954.

(15) Wright, J. W. IEEE Trans. Antennas and Propagation, vol. AP-16, pp. 217-223, March 1968.

(16) Cardone, V. J. Geophysical Science Laboratory, New York University, Report No. TR 69-1, December 1969.

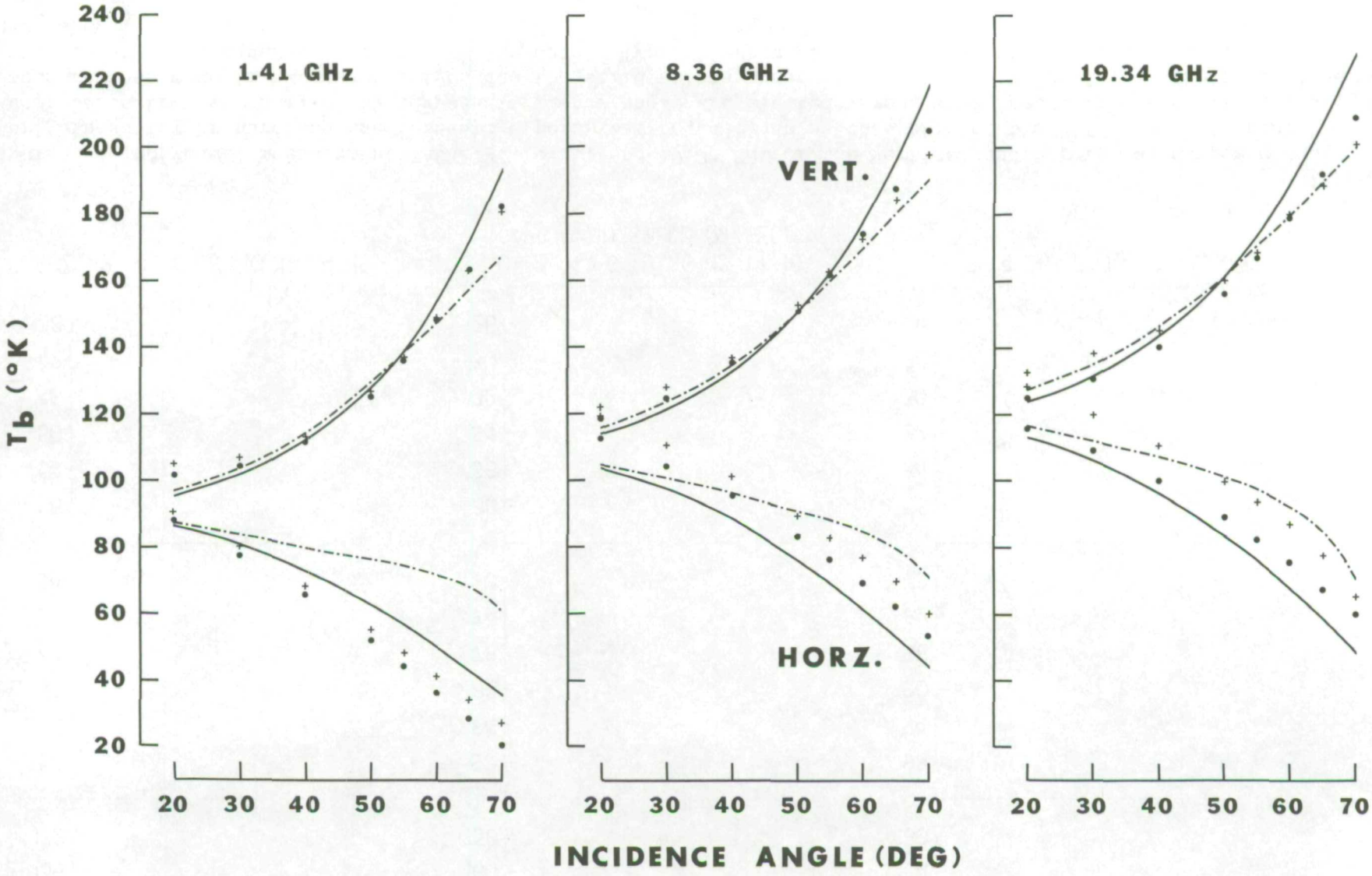

Figure 1.- The vertical and horizontal components of the brightness temperature of the sea at 1.41, 8.36, and 19.34 GHz are plotted as a function of incidence angle for two groups of measurements at the upper and lower ends of the wind speeds encountered. The dots and crosses are average measurements at 0.5 and 13.5 m/sec wind speeds respectively. The solid and dotted curves have been calculated for wind speeds of 0 and 15 m/sec respectively using the geometric optics model developed by Stogryn (1).

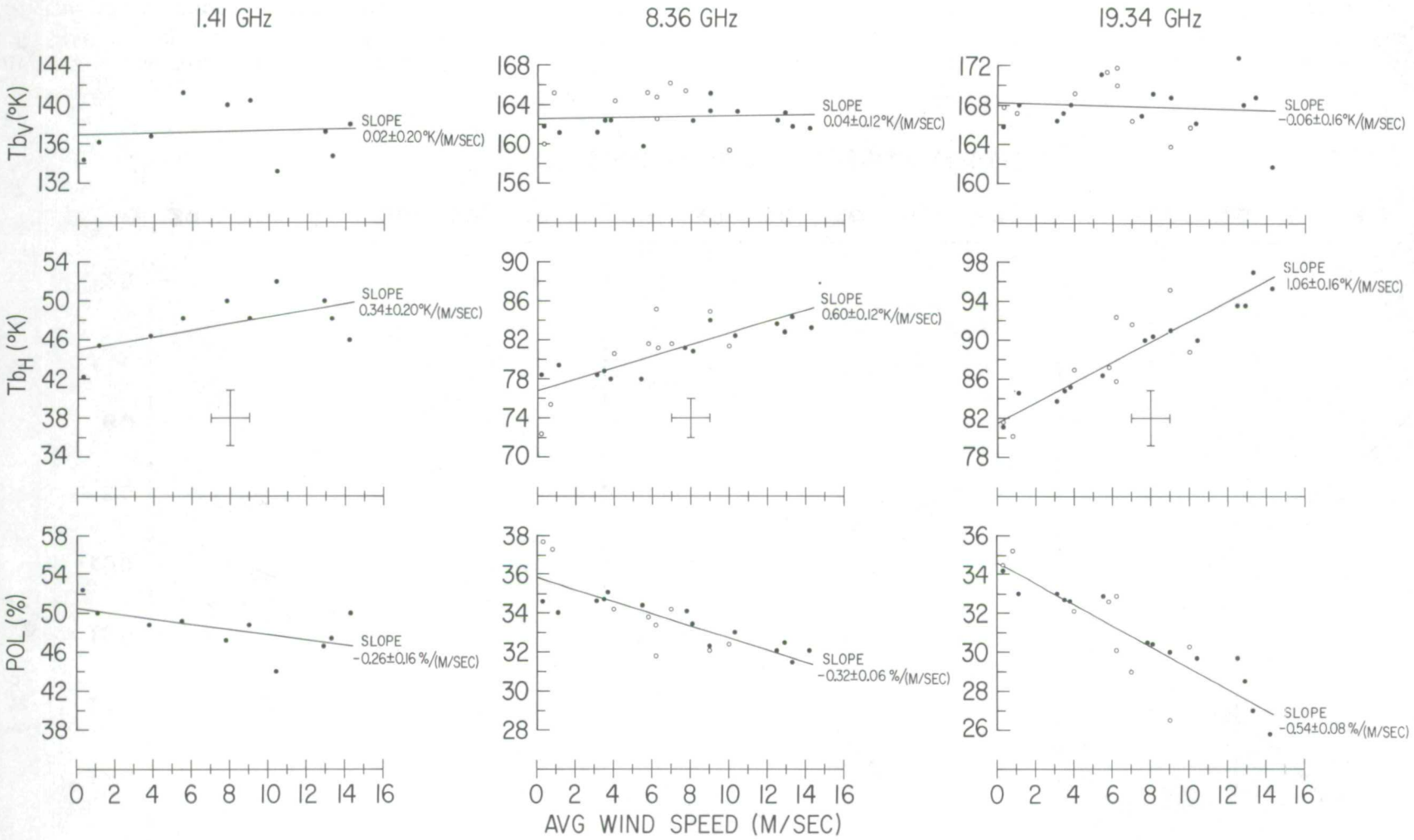

Figure 2.- Individual measurements at 1.41, 8.36, and 19.34 GHz of the vertical and horizontal components of brightness temperature and the percentage polarization, defined as the ratio of the difference of these two components to their sum, at 55 degrees incidence angle are plotted versus wind speed. The open circles are measurements made in March-April 1969 and the solid points observations made in March 1970. The solid lines are linear least-squares solutions to the data. Typical error bars applicable to the individual data points are shown.

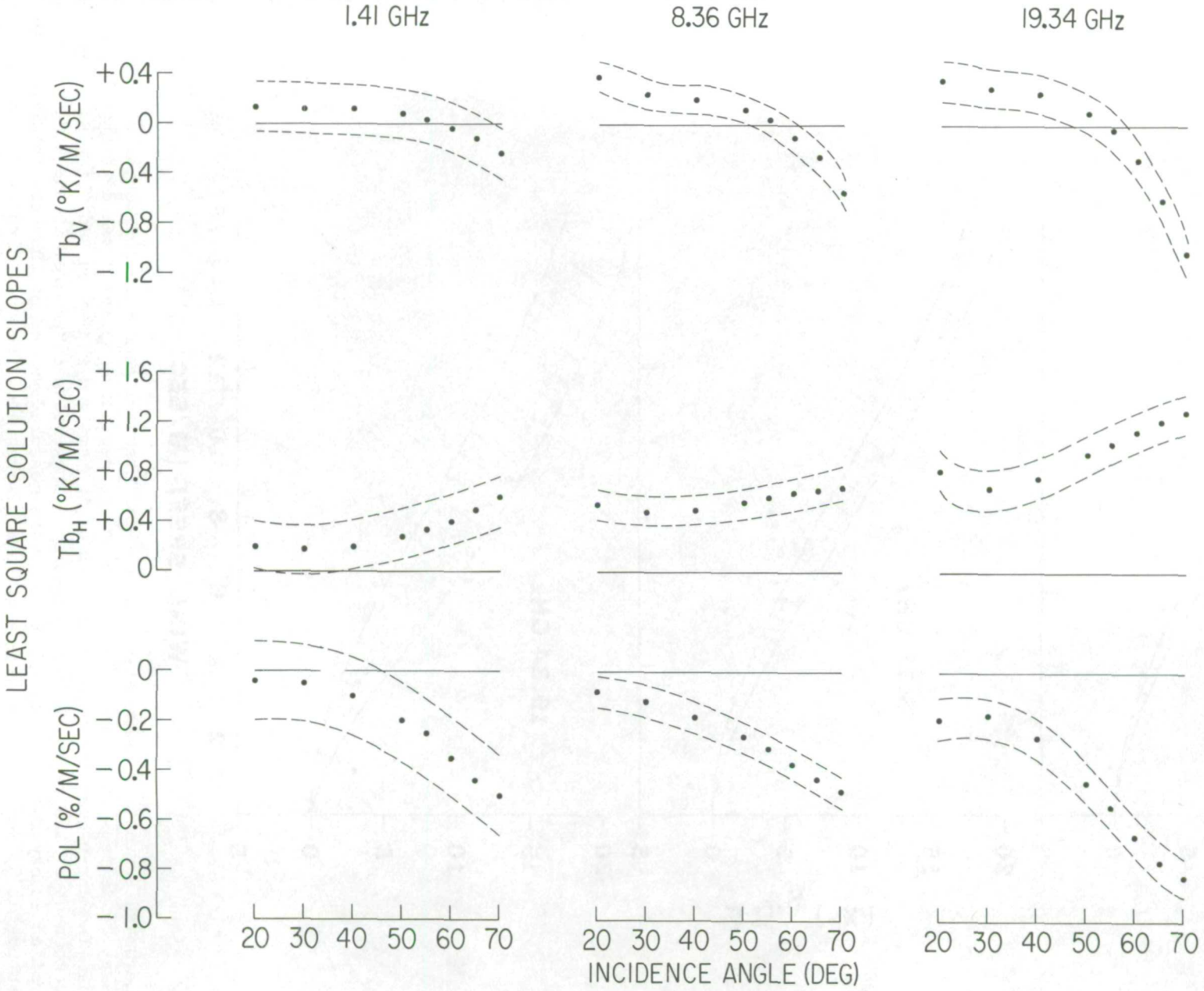

Figure 3.- The slopes of linear least-square solutions fitted to the measurements of the vertical and horizontal components of the brightness temperature and the percentage polarization at each incidence angle are plotted versus incidence angle. The dotted lines indicate the error in the slope determination.

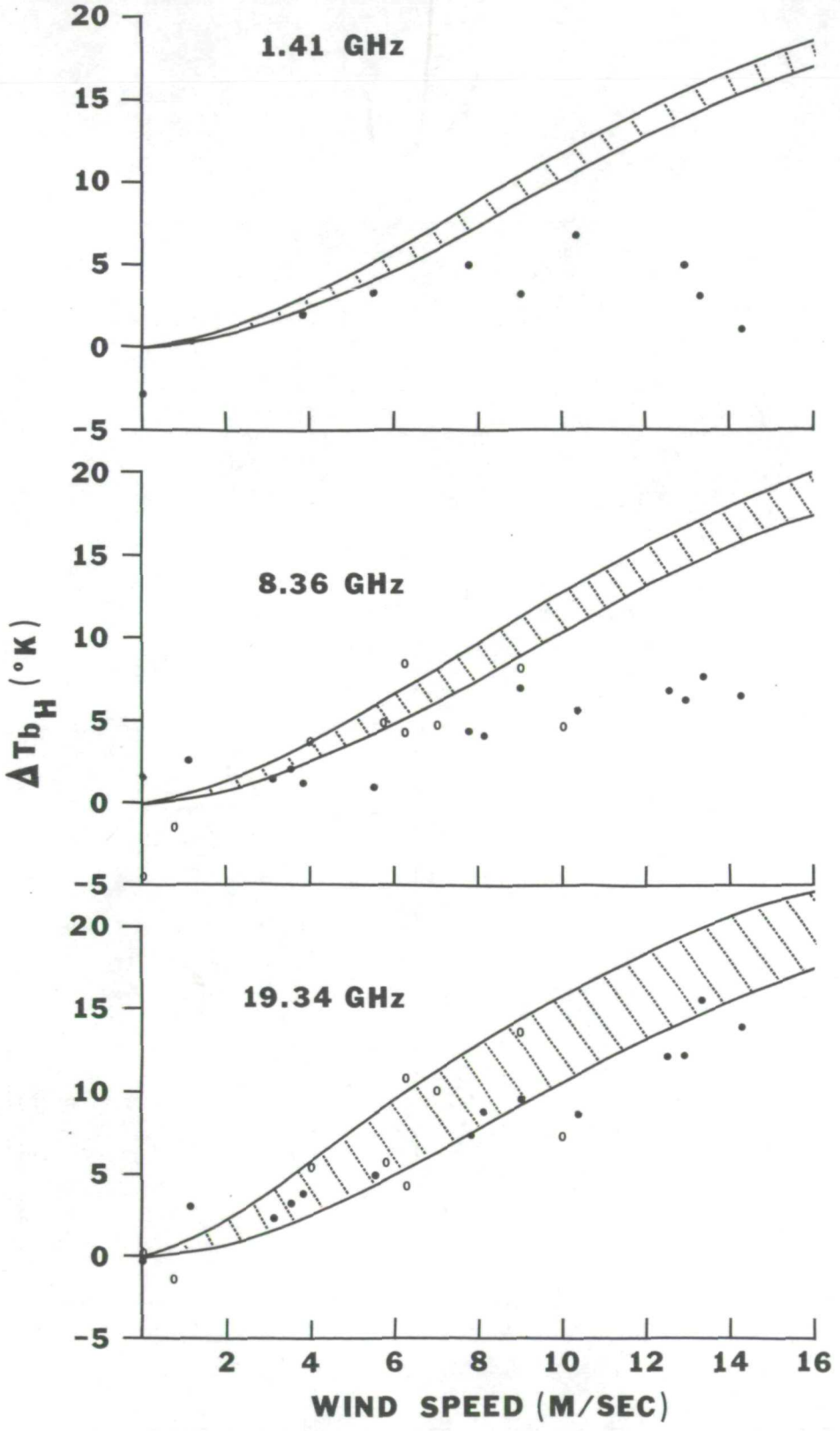

Figure 4.- The solid curves are calculations of the differential change in horizontal brightness temperature at 55 degrees incidence angle based on the geometric optics model developed by Stogryn (1). The upper curve represents the sum of the emitted radiation and the wind speed dependent component of the reflected sky radiation. The crosshatched area is the wind speed dependent reflected sky radiation contribution. The measured values of the horizontal brightness temperature at 55 degrees incidence angle are also shown. The open circles are March-April 1969 data and the solid points are measurements made in March 1970.